Available *online* at : http://jnte.ft.unand.ac.id/

Jurnal Nasional Teknik Elektro

| ISSN (Print) 2302-2949 | ISSN (Online) 2407-7267 |

Implementation of a PID-Based Temperature Control System on a Nextion HMI for Infant Warmer Applications

Farit Ardiyanto[*], *Slamet Pambudi*, *Joko Yunianto*

Sekolah Tinggi Teknologi Warga Surakarta, Indonesia

ARTICLE INFORMATION

Received: December 03, 2025
Revised: March 11, 2026
Accepted: March 27, 2026
Available online: March 29, 2026

KEYWORDS

embedded control, neonatal care, overshoot response, smart interface, thermal system

CORRESPONDENCE

Phone: +6281548354889
E-mail: farit@sttw.ac.id

A B S T R A C T

Infant body temperature stability is paramount, especially for preterm newborns unable to maintain their own thermal equilibrium. Here, we explore a Proportional-Integral-Derivative (PID) control algorithm implemented directly on a Nextion Human–Machine Interface (HMI) to regulate infant warmer temperature. Unlike typical systems where the microcontroller holds the major PID calculation and the HMI acts as a display only, this method integrates the PID logic into the HMI itself, with possible reductions of microcontroller load, minimization of communication delays, and hardware architecture simplification. Three trials at a constant setpoint of 37 °C with varying combinations of PID gains were used with a fixed experimental setup. Temperature response indicators like rise time, settling time, percent overshoot, and steady-state error were measured and compared. Results indicate that with gains of Kp = 1.50, Ki = 0.05, and Kd = 1.50, the system reached a steady state of 36.97 °C with just 2.16 % of an overshoot and a settling time of about 7 minutes and satisfied neonatal warmer requirements. The results confirm that PID control executed directly on the Nextion HMI can achieve temperature regulation performance comparable to conventional microcontroller-based implementations while improving system simplicity and code efficiency. It presents a good alternative choice of low-power and portable infant warmer and also of other embedded hot and cold control systems.

INTRODUCTION

Maintaining the body temperature of a newborn, especially premature or of low birth weight, is crucial for survival and also plays an important role in reducing both short-term and long-term health complications. However, hypothermia still occurs regularly even in most healthcare settings in tropical areas because such infants have immature temperature regulation, a large body surface area compared to their weight, and strict access to effective thermal care [1], [2], [3]. Recent findings confirm that the use of heating devices is effective in reducing hypothermia incidents, whether those based on electricity or low-cost alternatives do not compromise safety, given that the temperature falls within the physiological range of 36.5 °C until 37.5 °C [3], [4], [5], [6].

This approach represents the standard practice in well-resourced hospitals, but portable or low-power incubators are continually being developed for facilities with limited access to electricity [5], [6]. The design challenges related to incubators include temperature accuracy, power efficiency, and other environmental factors such as noise in incubators affecting infant comfort and sensory development. Low-noise incubator prototypes are being determined to have acoustic advantages with no compromise on thermal performance [7]. This also fosters mechatronic modeling of incubators and warmers with low-cost, open-source designs, understanding thermal dynamics, sensor integration, and pathways to implementation in low- and middle-income countries [8], [9]. While vision or thermography-based monitoring enables more detailed skin temperature assessment, it opens up opportunities for more adaptive closed-loop control [10].

It can be seen that, from the viewpoint of control, the only dominant industrial method is the Proportional-Integral-Derivative algorithm due to its simplicity and reliability in stabilizing systems with uncertainties and actuator limitations. Recent theoretical advances have further reinforced global and semi-global stability guarantees for PID of uncertain nonlinear systems, expanding the ranges of parameters and adopting modern antiwindup strategies in view of actuator saturation [11], [12], [13]. Process and manufacturing areas, including temperature control, are within the literature from 2021 to 2024. These works introduce improvements regarding model/data-based tuning, including autotuning-autotuning of fractional-order controllers-and performance comparison against advanced strategies, such as Model Predictive Control. Yet, PID remains an important strategy because of its low computational cost, robustness, and ease of implementation [14], [15], [16].

https://doi.org/10.25077/jnte.v15n1.1482.2026

Conventional architectures for medical devices bind the function of the main PID processor with an MCU, while the HMI serves only as an I/O interface [17]. While effective, this increases hardware complexity, serial communication traffic, and MCU workload. Advances in industrial HMI within the last five years including web-based and reconfigurable architectures revealed that control logic can be proxied closer to the plant by interface devices. Theoretical and empirical studies show that edge or on-device processing reduces latency, lowers bandwidth demand, and minimizes communication overhead-a factor critical to portable medical devices needing fast and deterministic thermal response [18], [19].

Building on these, one can run PID algorithms on HMIs directly if they come with scripting or embedded computing. This approach can reduce MCU workload, simplify device architecture and wiring, minimize serial communication latency, and easy to develop clinical interfaces if tuning, antiwindup, and saturation controls are designed properly [20], [21], [22]. In the light of both clinical and preclinical evidence, the requirement for thermal regulation devices-safe, portable, and energy-efficient-is huge [4], [7], [9] along with the advancement of non-contact temperature monitoring technologies [10].

However, most existing infant warmer control systems still rely on a conventional architecture where the PID control algorithm is executed entirely within the microcontroller, while the Human–Machine Interface (HMI) functions only as a display and user interaction device. Although this architecture has been widely adopted, it increases system complexity, requires continuous serial communication between devices, and places additional computational load on the microcontroller [23].

Recent advancements in industrial HMI technology have introduced scripting capabilities and embedded processing resources that allow certain control computations to be executed directly on the interface device. Despite this capability, the application of HMI-based control computation in medical thermal regulation systems has rarely been investigated [24]. Previous studies on infant warmers primarily focus on improving control strategies, such as PID tuning, fuzzy control, or hybrid controllers, but still maintain the microcontroller as the main control processor [25].

Therefore, a research gap exists regarding the feasibility and performance of implementing a PID control algorithm directly within an HMI platform for medical thermal regulation systems. The novelty of this study lies in demonstrating that the Nextion HMI can function not only as a visualization interface but also as the primary PID computation unit for infant warmer temperature control. This architectural approach has the potential to simplify hardware design, reduce communication latency, and decrease the computational workload on the microcontroller.

This paper aims at assessing the performance of implementing the PID algorithm on a Nextion HMI, keeping the temperature of an infant warmer at a set point of 37 °C, by evaluating metrics concerning dynamic response-rise time, settling time, overshoot, and steady-state error-and architectural considerations from the point of view of code efficiency and hardware simplicity in order to assess the viability of the strategy proposed for low-power portable neonatal devices.

The significance of this study lies in demonstrating a simplified control architecture for infant warmer systems by relocating the PID computation from the microcontroller to the Human–Machine Interface layer. This approach contributes to the development of compact and energy-efficient neonatal thermal regulation devices by reducing communication latency, simplifying hardware structure, and lowering the computational load of the microcontroller. In addition, this work provides experimental validation that HMI-based control execution can achieve thermal regulation performance comparable to conventional microcontroller-based PID controllers, thereby offering an alternative design strategy for portable medical devices.

METHODS

This study employed a quantitative experimental approach to evaluate the implementation of a PID control algorithm on a Nextion-based Human–Machine Interface for infant warmer temperature regulation. The experiment was conducted in the Laboratory of Electronics and Control at Sekolah Tinggi Teknologi Warga Surakarta and at PT. Entri Jaya Makmur, Surakarta. Three trial samples were carried out at a setpoint of 37 °C using different combinations of PID gains to observe the influence of Kp, Ki, and Kd on the system response.

PID Control Algorithm

This continuous-time PID control law is given by Equation 1, with K_p, K_i, and K_d being the gains of the proportional, integral, and derivative terms, respectively. In order to implement this controller in Nextion HMI, a discretization was performed using a fixed period of sampling of 250 ms, arriving at the discrete form shown in Equation 2.

$$u(t) = K_p\, e(t) \;+\; K_i \int e(t)\, dt \;+\; K_d\, \frac{de(t)}{dt} \tag{1}$$

Where *Kp* is the proportional gain, which scales the control output in direct proportion to the temperature error, *Ki* is the integral gain eliminating the steady-state error by summing up past errors over time, and *Kd* is the derivative gain, predicting future error trends, therefore helping to damp overshoot and aiding transient response.

$$u(k) \;=\; u(k-1) \;+\; Kp(e(k) \;-\; e(k-1)) \;+\; Ki \cdot e(k) \cdot \Delta t \\ +\; \left(\frac{Kd}{\Delta t}\right)\big(e(k) -\; 2e(k-1) +\; e(k-2)\big) \tag{2}$$

This discretization allows efficient computation within the HMI's scripting environment without external microcontroller processing [26]

a) Error Differences

Equation 3 is the first-order error change that represents how much the current sample differs from the previous sample. Thus,

https://doi.org/10.25077/jnte.v15n1.1482.2026

Equation 4 represents the second order of error difference that reflects the acceleration of the error variation.

$$dE_1[k] = e[k] - e[k-1] \quad (3)$$

Formula: dE1[k]=e[k]-e[k-1]
HMI Code:
vDE1.val=vE.val
vDE1.val=vDE1.val-vE1.val

$$dE_2[k] = e[k] - 2e[k-1] + e[k-2] \quad (4)$$

Formula: d2E[k]=e[k]-2e[k-1]+e[k-2]
HMI Code:
vD2E.val=vE.val
vD2E.val=vD2E.val-vE1.val
vD2E.val=vD2E.val-vE1.val
vD2E.val=vD2E.val+vE2.val

b) Proportional Term

Equation 5 defines the proportional term, where the control output is obtained by multiplying the proportional gain K_p with the first-order error difference $dE_1[k]$

$$P[k] = K_p \cdot dE_1[k] \approx \frac{K_p\, s \cdot dE_1}{s} \quad (5)$$

Formula: P[k]=Kp·dE1[k] ≈ (KpS·dE1)/S
HMI Code:
vTmp.val=vKpS.val
vTmp.val=vTmp.val*vDE1.val
vP.val=vTmp.val/vS.val

c) Integral Term

Equation 6 defines the integral term, where the accumulated error over time is multiplied by the integral gain K_i and the sampling period Δt, providing the corrective action needed to eliminate steady-state error.

$$I[k] = K_i \cdot e[k] \cdot \Delta t \approx \frac{K_i\, S \cdot e \cdot \Delta t_{ms}}{S \cdot 1000} = \frac{K_i\, S \cdot e \cdot \Delta t_{ms}}{vDen} \quad (6)$$

Formula: I[k]=Ki·e[k]·Δt ≈ (KiS·e·Δt_ms)/(S·1000)=(KiS·e·Δt_ms)/vDen
HMI Code:
vTmp.val=vKiS.val
vTmp.val=vTmp.val*vE.val
vTmp.val=vTmp.val*vDtMs.val
vI.val=vTmp.val/vDen.val

d) Derivative Term

The derivative term described by Equation.7 predicts the future trend of the error, multiplying the second-order difference of an error with derivative gain Kd and a sampling interval Δt, thus assisting in the enhancement of the system stability and reduction of overshooting.

$$D[k] = Kd \cdot \Delta t \cdot d2E[k] \approx \frac{Kd\, S \cdot \Delta t_{ms} \cdot d2E}{S \cdot 1000} = \frac{Kd\, S \cdot \Delta t_{ms} \cdot d2E}{vDen} \quad (7)$$

Formula: D[k]=Kd·Δt·d2E[k] ≈ (KdS·Δt_ms·d2E)/(S·1000)=(KdS·Δt_ms·d2E)/vDen
HMI Code:
vTmp.val=vKdS.val
vTmp.val=vTmp.val*vDtMs.val
vTmp.val=vTmp.val*vD2E.val
vD.val=vTmp.val/vDen.val

e) Output Accumulation

In this approach, the final control action is computed by accumulating the previous output together with the P, I, and D terms, as described in Equation 8.

$$u[k] = u[k-1] + P[k] + I[k] + D[k] \quad (8)$$

Formula: u[k]=u[k-1]+P[k]+I[k]+D[k]
HMI Code:
vU.val=vU1.val
vU.val=vU.val+vP.val
vU.val=vU.val+vI.val
vU.val=vU.val+vD.val

f) Anti Wind-Up

To prevent integrator wind-up, an additional feedback term is introduced, as formulated in Equation 9, where the anti-windup gain K_{aw} compensates for the difference between the saturated and pre-saturated control signals.

$$\dot{I}(t) = K_i\, e(t) + K_{aw}\,(u_{sat}(t) - u_{pre}(t)) \quad (9)$$

Formula: I[k]=I[k−1]+(Kie[k]+Kaw(usat[k]−upre[k]))Δt
HMI Code:

```
if(nKp.val>0)
{
 vaKaw.val=nKi.val*vaS.val
 vaKaw.val=vaKaw.val/nKp.val
}else
{
 vaKaw.val=0
}
vaTmp1.val=vaU.val-vaUuns.val
vaTmp2.val=vaKaw.val*vaTmp1.val
vaTmp4.val=vaTmp2.val/vaS.val
```

g) History Update

To maintain accurate recursive computation, the control output and error terms are updated as shown in Equation 10, where past values are shifted to store the most recent samples.

$$u[k-1] \leftarrow u[k];\ e[k-2] \leftarrow e[k-1];\ e[k-1] \leftarrow e[k] \quad (10)$$

Formula: u[k-1]←u[k]; e[k-2]←e[k-1]; e[k-1]←e[k]
HMI Code:
vU1.val=vU.val
vE2.val=vE1.val
vE1.val=vE.val
vU.val=0

System Configuration

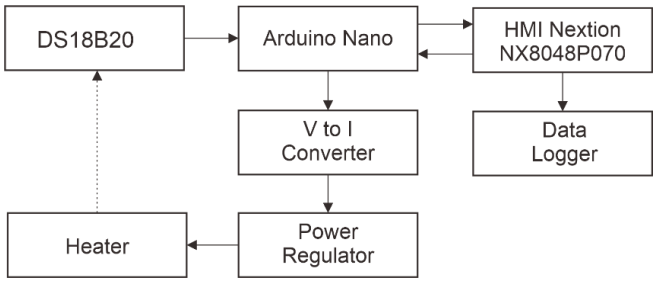

Figure 1. System Block Diagram

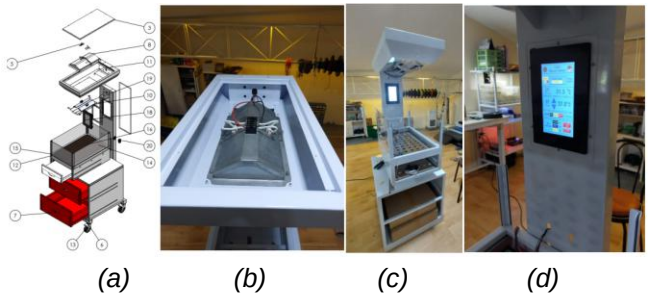

Figure 2. Hardware Prototype (a) Exploded View Of The Infant Warmer Assembly, (b) Heating Unit With Reflector And Mounted Heating Element, (c) Complete Prototype Of The Infant Warmer Structure, (d) Nextion HMI Panel For Temperature Control And Monitoring

Figure 1 shows the proposed system architecture where the HMI performs the PID and the MCU actuates the actuator, and Figure 2 is the hardware prototype photograph of the infant warmer controller. For the experiment, the setup involved a temperature sensor, DS18B20 that would provide accurate thermal measurement. The Nextion HMI was programmed for the implementation of PID and simultaneously displaying the temperature measurements. The calculated output from the HMI was sent to an Arduino, which converted the signal into a PWM signal and supplied it to a voltage-to-current converter module. This is because the power regulator acting as a heater driver was designed to accept only current input. Temperature data were saved periodically in the EEPROM of the HMI. Figure 1 shows the block diagram of the proposed system, where the Nextion HMI is acting both as display and PID processor, hence communicating with the microcontroller only for actuator control [27].

Data Collection Procedure

Data sampling was done every 10 seconds. This range was adopted because during temperature PID, changes are not fast. Therefore, if the time sampling is too low, many records will be the same, which is inefficient. The 10-second range is also used to save memory. This is very important because the result of the experiments is stored in EEPROM available on the HMI with the maximum capacity of 1024 bytes; 850 bytes are allocated for the temperature stored, and the rest is used for other purposes. By setting up this kind of setup, since each record of temperature uses 4 bytes, it can record up to 212 data. The number of recorded data means recording time is 2120 second or approximately 35 minutes.

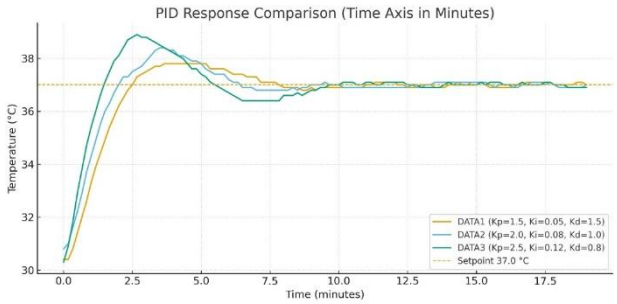

Figure 3. Data logging timeline (10 s interval) and setpoint profile at 37 °C, with markers for Sample-1 to Sample-3.

Figure 3 shows the 10 second logging timeline at fixed 37 °C setpoint and the sequence of the three PID tunings.

1. The prototype infant warmer initialized, the temperature setpoint was fixed at 37 °C. Three sets of PID gains were applied sequentially to the HMI: Sample 1: (1.50, 0.05, 1.50) ; Sample 2: (2.00, 0.08, 1.00) ; Sample 3: (2.50, 0.12, 0.80)
2. The temperature response, thereafter, is recorded every 10 seconds using internal data logging of the HMI.
3. Key performance indicators rise time, settling time, percentage overshoot, steady-state error, and temperature ripple were calculated for each trial.

Data Analysis

Descriptive statistics of the captured temperature records were calculated. Response curves were plotted to compare dynamic behavior across different PID gain settings. Results were also compared against the standard neonatal thermal stability requirements to assess medical suitability classes [28], [29]. This approach offers a structured way to establish whether the direct implementation of PID on an HMI performs comparably to, or outperforms, the conventional microcontroller-based designs by reducing hardware complexity and enhancing energy efficiency.

RESULTS AND DISCUSSION

Overview of Experimental Data

The experiments involved a set point of 37 °C, with sampling done from time to time using the Nextion HMI, which also implemented the PID algorithm. Temperature recordings were made at regular intervals to measure rise time, settling time,

https://doi.org/10.25077/jnte.v15n1.1482.2026

percentage overshoot, and steady-state error. Three trials, Sample-1 to Sample-3, were prepared by changing Kp, Ki, and Kd, as described in the methodology.

The experimental results demonstrate that the PID temperature controller implemented directly on the Nextion HMI is capable of maintaining thermal stability within the required neonatal temperature range. Among the three tested configurations, the PID parameter set Kp = 2.00, Ki = 0.08, and Kd = 1.00 (Sample-2) provides the most balanced performance, achieving a fast dynamic response with moderate overshoot and the lowest cumulative control error. This result indicates that executing the PID algorithm directly on the HMI does not degrade the control performance compared with conventional microcontroller-based architectures while offering advantages in system simplicity and reduced communication overhead.

Temperature Response for Sample-1 until Sample-3

Table 1. Comparative Dynamic-Response Metrics For Three PID Tuning Sets (SP = 37 °C).

Data	Kp–Ki–Kd	t_rise 10–90%	Overshoot (°C / %)	t_settle (±2% SP)	SS error (≈last 30 samples)	IAE (°C·s)
Sample-1 (DATA1)	1.50–0.05–1.50	~100 s	0.8 / 2.16%	~320 s	-0.033 °C	744
Sample-2 (DATA2)	2.00–0.08–1.00	~90 s	1.4 / 3.78%	~310 s	+0.010 °C	644
Sample-3 (DATA3)	2.50–0.12–0.80	~60 s	1.9 / 5.14%	~280 s	+0.010 °C	717

Table 1 shows Sample 1, which was very conservative and well-damped, this meant very little overshoot, but this came at the price of a slower convergence. Sample 2 provided the best balance between a fairly quick response and moderate overshoot and, thus, the lowest cumulative error. Sample 3 gave the quickest response time but with the highest overshoot. These results point out that there is a dilemma in how increasing the response speed of a PID-controlled thermal system would lead to less stability; thus, parameter tuning needs to be done based on specific requirements posed by either clinical or application-driven demands.

When compared with previously reported infant warmer temperature control systems, the dynamic response obtained in this study is comparable to existing PID-based or hybrid control approaches. For example, previous work on PID-controlled infant warmers reported settling times within several minutes depending on the tuning configuration [30], while hybrid fuzzy–PID control systems achieved improved stability but required more complex computational processing [29]. The settling times obtained in this study (approximately 280–320 seconds) fall within the same operational range while maintaining low steady-state error and limited overshoot.

These results suggest that executing the PID algorithm directly on the Nextion HMI can achieve thermal control performance comparable to conventional microcontroller-based implementations. At the same time, the proposed architecture offers potential advantages in terms of reduced system complexity, simplified communication structure, and improved suitability for compact or portable neonatal thermal devices.

Comparative Analysis Across PID Settings

Speed-rise and settling performance follow the order Sample-3 < Sample-2 < Sample-1, indicating that Sample-3 produces the fastest response. Overshoot is lowest in Sample-1, moderate in Sample-2, and highest in Sample-3. In terms of steady-state accuracy, Sample-2 and Sample-3 show a very small positive bias of approximately +0.010 °C, whereas Sample-1 presents a slight negative bias of −0.033 °C. For integral performance, the IAE value is lowest in Sample-2, indicating the best overall efficiency, followed by Sample-3 and lastly Sample-1.

Implied action: Sample-2 represents a balanced operating point; Sample-3 is used when fastest settling is needed/required, tolerating ≈5% overshoot; and Sample-1 when overshoot must be at its minimum. Table 1. Comparing PID performance for three sets of parameters (SP = 37.0 °C). trise = 10–90% uptime tsettle = time of default on the band ±2% SP; SS error = Steady-State Error (last ≈30 samples)

CONCLUSION

This study demonstrates that a PID control algorithm can be successfully implemented directly within a Nextion HMI to regulate the temperature of an infant warmer system at the clinical setpoint of 37 °C. Experimental results show that the HMI-based PID controller is capable of maintaining stable thermal regulation with dynamic response characteristics comparable to conventional controller architectures, including low steady-state error (≈ –0.033 °C for Sample 1 and ≈ +0.010 °C for Samples 2/3), limited overshoot (≈ 2.16% in conservative tuning), and settling times of approximately 280–320 seconds (≈ 4.7–5.3 minutes) within the ±2% stability band. These findings indicate that executing the PID algorithm directly on the HMI can achieve reliable temperature control while supporting simplified system architecture for infant warmer applications.

Also, making the HMI the main processor reduces communication latency and simplifies the overall system architecture. Thus, it is promising for compact low-power portable devices, in line with edge/IoMT literature highlighting deterministic response and bandwidth efficiency [31], whereas a web-based/reconfigurable HMI simplifies updates to the interface itself [21], [32].

The implemented back-calculation/clamping scheme effectively avoided integral windup during saturation, reducing overshoot and accelerating settling [20], [22], in agreement with the stability framework reported [11] and hierarchical design .

For comparison, Sample 2 (Kp = 2.00, Ki = 0.08, Kd = 1.00) provides the best performance trade-off—balanced cumulative error (IAE), a moderate overshoot, and close to zero steady-state bias. Sample 3 is preferable for the fastest possible rise and settling and ≈5% overshoot, whereas Sample 1 is recommended when the overshoot has to be minimal. Further work will consider the extension of robustness testing, long-term reliability, and

direct validation against classical MCU-based PID to further consolidate the proposed HMI-based approach. Based on a simple model, conservative tuning refined by IAE/ITAE proves to be a practical compromise between speed and overshoot [12], [14], [15], [33]. Although MPC clearly outperforms conventional controllers when dealing with complex constraints, PID is still competitive thanks to its low computational cost and is well-suited for on-device HMI platforms [31], [34].

From an architectural perspective, the proposed HMI-based PID control approach provides an alternative design paradigm for embedded medical devices. By allowing the HMI to execute the control algorithm, the system architecture becomes simpler and potentially more energy-efficient, which is particularly beneficial for portable neonatal care equipment intended for healthcare environments with limited infrastructure.

ACKNOWLEDGMENT

This research received funding from the Directorate General of Research and Development, Ministry of Higher Education, Science, and Technology, as stated in the official Research Contract for the Fiscal Year 2025.

The authors extend their appreciation to Dr. Ir. Musabbikhah, S.T., M.T., and the Research and Community Service Center of Sekolah Tinggi Teknologi Warga Surakarta for their guidance and institutional support provided in accordance with the Penelitian Dosen Pemula Research Contract, Fiscal Year 2025.

The authors also express their sincere gratitude to PT. Entri Jaya Makmur for the technical assistance, laboratory access, and valuable support offered throughout the development and experimental testing of the prototype.

REFERENCES

[1] M. N. Cramer, D. Gagnon, O. Laitano, and C. G. Crandall, "Human Temperature Regulation Under Heat Stress in Health, Disease, and Injury," *Physiol. Rev.*, vol. 102, no. 4, pp. 1907–1989, 2022, doi: 10.1152/PHYSREV.00047.2021.

[2] E. A. Dunne, C. P. F. O'Donnell, B. Nakstad, and L. K. McCarthy, "Thermoregulation for very preterm infants in the delivery room: a narrative review," *Pediatr. Res.*, vol. 95, no. 6, pp. 1448–1454, 2024, doi: 10.1038/s41390-023-02902-w.

[3] M. Kyokan, N. Bochaton, V. Jirapaet, and R. E. Pfister, "Early detection of cold stress to prevent hypothermia: A narrative review," *SAGE Open Med.*, vol. 11, 2023, doi: 10.1177/20503121231172866.

[4] J. Uwamariya *et al.*, "Safety and effectiveness of a non-electric infant warmer for hypothermia in Rwanda: A cluster-randomized stepped-wedge trial," *EClinicalMedicine*, vol. 34, p. 100842, 2021, doi: 10.1016/j.eclinm.2021.100842.

[5] N. D. P. Bluhm *et al.*, "Preclinical validation of NeoWarm, a low-cost infant warmer and carrier device, to ameliorate induced hypothermia in newborn piglets as models for human neonates," *Front. Pediatr.*, vol. 12, no. April, pp. 1–11, 2024, doi: 10.3389/fped.2024.1378008.

[6] U. Mishra, D. August, K. Walker, P. R. Jani, and M. Tracy, "Thermoregulation, incubator humidity, and skincare practices in appropriate for gestational age ultra-low birth weight infants: need for more evidence," *World Journal of Pediatrics*, vol. 20, no. 7, pp. 643–652, 2024, doi: 10.1007/s12519-024-00818-x.

[7] R. Hernández-Molina, V. Puyana-Romero, J. L. Beira-Jiménez, A. Morgado-Estévez, R. Bienvenido-Bárcena, and F. Fernández-Zacarías, "Silent Neonatal Incubators, Prototype Nica+," *Acoustics*, vol. 6, no. 3, pp. 638–650, 2024, doi: 10.3390/acoustics6030035.

[8] A. R. Casado, M. Larrodé-Díaz, F. F. Zacarias, and R. H. Molina, "Experimental and computational model for a neonatal incubator with thermoelectric conditioning system," *Energies (Basel).*, vol. 14, no. 17, pp. 1–16, 2021, doi: 10.3390/en14175278.

[9] R. Cuervo, M. A. Rodríguez-Lázaro, R. Farré, D. Gozal, G. Solana, and J. Otero, "Low-cost and open-source neonatal incubator operated by an Arduino microcontroller," *HardwareX*, vol. 15, no. July, 2023, doi: 10.1016/j.ohx.2023.e00457.

[10] S. Lyra *et al.*, "Camera fusion for real-time temperature monitoring of neonates using deep learning," *Med. Biol. Eng. Comput.*, vol. 60, no. 6, pp. 1787–1800, 2022, doi: 10.1007/s11517-022-02561-9.

[11] C. Zhao and L. Guo, "Towards a theoretical foundation of PID control for uncertain nonlinear systems," *Automatica*, vol. 142, p. 110360, Aug. 2022, doi: 10.1016/j.automatica.2022.110360.

[12] E. Hernández-Arroyo, J. L. Díaz-Rodríguez, and O. Pinzón-Ardila, "Estudio del comportamiento de un Control MPC [Control Predictivo Basado en el Modelo] comparado con un Control PID en una Planta de Temperatura," *Revista Facultad De Ingeniería*, vol. 23, no. 37, p. 45, 2014, doi: 10.19053/01211129.2789.

[13] J. Zhang, C. Zhao, and L. Guo, "On PID Control Theory for Nonaffine Uncertain Stochastic Systems," *J. Syst. Sci. Complex.*, vol. 36, no. 1, pp. 165–186, Feb. 2023, doi: 10.1007/s11424-022-1486-9.

[14] Z. Li, "Review of PID control design and tuning methods," *J. Phys. Conf. Ser.*, vol. 2649, no. 1, p. 012009, Nov. 2023, doi: 10.1088/1742-6596/2649/1/012009.

[15] M. Ghita *et al.*, "A robust self-tuning PID-type control for time-varying process in the pharmaceutical industry," in *2022 13th Asian Control Conference (ASCC)*, IEEE, May 2022, pp. 637–642. doi: 10.23919/ASCC56756.2022.9828229.

[16] F. Ardiyanto, W. Wiyono, R. Rahmat, and E. B. Raharjo, "Design and manufacturing of control circuits for centrifuge device motors," *BIS Energy and Engineering*, vol. 1, p. V124016, Nov. 2024, doi: 10.31603/biseeng.42.

[17] F. Ardiyanto, Wiyono, and Rahmat, "Design and build LCD touchscreen (HMI) as a controller and indicator on biological safety cabinet machines to protect workers from virus exposure," 2023, p. 020103. doi: 10.1063/5.0120936.

https://doi.org/10.25077/jnte.v15n1.1482.2026

[18] M. Huba, S. Chamraz, P. Bistak, and D. Vrancic, "Making the PI and PID Controller Tuning Inspired by Ziegler and Nichols Precise and Reliable," *Sensors*, vol. 21, no. 18, p. 6157, Sep. 2021, doi: 10.3390/s21186157.

[19] E. Fridman and A. Selivanov, "Using Delay for Control," *Annu. Rev. Control Robot. Auton. Syst.*, vol. 8, no. 1, pp. 101–126, 2025, doi: 10.1146/annurev-control-022723-033031.

[20] X. Zhang, S. Xi, and J. Zhang, "Anti-Windup Method Using Ancillary Flux-Weakening for Enhanced Induction Motor Performance Under Voltage Saturation," *Electronics (Switzerland)*, vol. 14, no. 17, pp. 1–17, 2025, doi: 10.3390/electronics14173496.

[21] L. Liu, Z. Xu, and X. Qu, "A Reconfigurable Architecture for Industrial Control Systems: Overview and Challenges," *Machines*, vol. 12, no. 11, p. 793, Nov. 2024, doi: 10.3390/machines12110793.

[22] C.-W. Chen, H.-M. Wu, and C.-Y. Nian, "A Class of Anti-Windup Controllers for Precise Positioning of an X-Y Platform with Input Saturations," *Electronics (Basel).*, vol. 14, no. 3, p. 539, Jan. 2025, doi: 10.3390/electronics14030539.

[23] M. Mahmud, S. M. A. Motakabber, A. H. M. Zahirul Alam, and A. N. Nordin, "Adaptive PID Controller Using for Speed Control of the BLDC Motor," in *IEEE International Conference on Semiconductor Electronics, Proceedings, ICSE*, Institute of Electrical and Electronics Engineers Inc., Jul. 2020, pp. 168–171. doi: 10.1109/ICSE49846.2020.9166883.

[24] Y. Wang, Z. Jiang, S. H. Kwon, M. Ibrahim, A. Dang, and L. Dong, "Flexible Sensor-Based Human–Machine Interfaces with AI Integration for Medical Robotics," *Advanced Robotics Research*, vol. 2, no. 1, Feb. 2026, doi: 10.1002/adrr.202500027.

[25] R. Kristiyono and Wiyono, "Autotuning fuzzy PID controller for speed control of BLDC motor," *Journal of Robotics and Control (JRC)*, vol. 2, no. 5, pp. 400–407, Sep. 2021, doi: 10.18196/jrc.25114.

[26] M. A. Mohammed, M. Khamees, and D. H. Abbas, "Automatic Temperature Control System Using African vultures optimization algorithm," *Iraqi Journal for Computer Science and Mathematics*, vol. 5, no. 3, Jan. 2024, doi: 10.52866/ijcsm.2024.05.03.044.

[27] M. Dwi Mubarok, M. Sofie, and M. Rofii'i, "Kontrol Infant Warmer Dilengkapi Baterai Dan Inverter," *MEDIKA TRADA*, vol. 6, no. 1, pp. 36–41, Jun. 2025, doi: 10.59485/jtemp.v6i1.122.

[28] A. Majid *et al.*, "Comparative Analysis of PID and Fuzzy Temperature Control System on Infant Warmer (Control PID)," *Journal of Electronics, Electromedical Engineering, and Medical Informatics*, vol. 4, no. 4, pp. 223–228, 2022, doi: 10.35882/ijahst.v4i4.257.

[29] A. Alimuddin, R. Arafiyah, I. Saraswati, R. Alfanz, P. Hasudungan, and T. Taufik, "Development and Performance Study of Temperature and Humidity Regulator in Baby Incubator Using Fuzzy-PID Hybrid Controller," *Energies (Basel).*, vol. 14, no. 20, p. 6505, Oct. 2021, doi: 10.3390/en14206505.

[30] I. Sharma and M. Singh, "Infant Warmer Design with PID Control for Stability and Equal Temperature Distribution Equipped with Digital Scales for Prevention of Hypothermia in Newborns," *International Journal of Advanced Health Science and Technology*, vol. 1, no. 1, pp. 7–13, Oct. 2021, doi: 10.35882/ijahst.v1i1.2.

[31] K. Alatoun, K. Matrouk, M. A. Mohammed, J. Nedoma, R. Martinek, and P. Zmij, "A Novel Low-Latency and Energy-Efficient Task Scheduling Framework for Internet of Medical Things in an Edge Fog Cloud System," *Sensors*, vol. 22, no. 14, 2022, doi: 10.3390/s22145327.

[32] S.-L. Jeng, W.-H. Chieng, and Y. Chen, "Web-Based Human-Machine Interfaces of Industrial Controllers in Single-Page Applications," *Mobile Information Systems*, vol. 2021, pp. 1–13, Apr. 2021, doi: 10.1155/2021/6668843.

[33] C. I. Muresan, I. Birs, C. Ionescu, E. H. Dulf, and R. De Keyser, "A Review of Recent Developments in Autotuning Methods for Fractional-Order Controllers," *Fractal and Fractional*, vol. 6, no. 1, 2022, doi: 10.3390/fractalfract6010037.

[34] X. Wang *et al.*, "Empowering Edge Intelligence: A Comprehensive Survey on On-Device AI Models," *ACM Comput. Surv.*, vol. 57, no. 9, pp. 1–39, Sep. 2025, doi: 10.1145/3724420.

NOMENCLATURE

T	Measured temperature (°C)
Tset	Temperature setpoint (°C)
e(k)	Temperature error at sample k
u(k)	Control output at sample k
u(k−1)	Previous control output
Δt	Sampling period (s or ms)
trise	Rise time (10–90%) of temperature response
tsettle	Settling time within ±2% of setpoint
SS error	Steady-state error
IAE	Integral of Absolute Error (°C·s)
Kp	Proportional gain
Ki	Integral gain
Kd	Derivative gain
dE1[k]	First-order error difference: e(k) − e(k−1)
d2E[k]	Second-order error difference: e(k) − 2e(k−1) + e(k−2)
P[k]	Proportional term at sample k
I[k]	Integral term at sample k
D[k]	Derivative term at sample k
Kaw	Anti-windup gain
usat[k]	Saturated control output
upre[k]	Pre-saturated control output

AUTHOR(S) BIOGRAPHY

Farit Ardiyanto is a permanent lecturer in the S1 Electrical Engineering Program at Sekolah Tinggi Teknologi Warga Surakarta. His research interests include electronic control systems, industrial electronics, and instrumentation, with a focus on embedded and automated control applications.

Slamet Pambudi is a permanent lecturer in the S1 Electrical Engineering Program at Sekolah Tinggi Teknologi Warga Surakarta. His academic and research activities center on programmable logic controllers (PLC), industrial automation, and applied instrumentation.

Joko Yunianto is a permanent lecturer in the D3 Mechanical Engineering Program at Sekolah Tinggi Teknologi Warga Surakarta. His research focuses on fluid system engineering and practical applications of thermofluid mechanics in industrial systems.

https://doi.org/10.25077/jnte.v15n1.1482.2026